Proceedings of the 17th World Congress
The International Federation of Automatic Control
Seoul, Korea, July 6-11, 2008

Nonlinear Control of Full-Vehicle Active Suspensions with Backstepping Design Scheme

Jia-Wei Hu * **Jung-Shan Lin** **

* *Department of Electrical Engineering, National Chi Nan University, Taiwan 545, R.O.C. (Tel:049-2910960-4856; e-mail: s94323545@ncnu.edu.tw).*
** *Department of Electrical Engineering, National Chi Nan University, Taiwan 545, R.O.C. (Tel:049-2910960-4801; e-mail: jslin@ncnu.edu.tw).*

Abstract: This paper proposes a nonlinear backstepping control strategy to improve the inherent tradeoff between ride comfort of passengers and suspension travel. Passenger comfort in ground vehicles usually depends on a combination of vertical motion (heave) and angular motion (pitch and roll). Suspension travel means the space variation between vehicle body and tires. Our active suspension design has the ability to cope with these two conflicting objectives for improving the tradeoff between them. The novelty is in use of the nonlinear filter whose effective bandwidth depends on the magnitudes of suspension travel. Hence, the nonlinear design allows the closed-loop system to behave differently in various operating regions. As a result, the excellent performance of full-vehicle active suspension is demonstrated in simulations compared to a standard passive suspension system.

1. INTRODUCTION

The control design of active suspension systems has been one of the favorite subjects in automotive research area. The advantages of active suspensions have been also promised for many years. According to its ability for the utilization of extracting energy, a suspension system can be classified as passive, semi-active and active.

Passive suspension systems in Miller (1998) and Karmopp (1992) include the conventional springs and shock absorber used in most vehicles. Current automobile suspension systems using passive components can only offer a compromise between these two conflicting criteria by providing spring and damper coefficients with fixed rates.

Semi-active suspensions in Paulides (2006) provide controlled real-time dissipation of energy. For an automotive suspension system, this is achieved through a mechanical device called an active damper. The main feature of this system is the ability to adjust the damping of suspension system without any use of actuators. This type of system requires some form of measurement with a controller board in order to properly tune the damping.

Active suspension shown in Esmailzadh (1996); Huang (2004); Lin (2004, 2007); Sam (2000); Thomson (2001) employs pneumatic or hydraulic actuators which in turn create the desired force in the suspension systems. The performance of a vehicle suspension system is evaluated by providing improved the ride comfort of passengers and avoiding hitting its suspension travel limits. Even if the traditional passive suspension system can effectively negotiate this tradeoff, the active suspension systems still have better performance and other advantages than passive ones. For instance, the active suspension systems not only can effectively emphasize the ride quality and handling performance, but also obtain the secondary benefits of better braking and cornering because of reduced weight transfer.

The nonlinear backstepping design has been applied to quarter-car and half-car active suspension systems in Lin (1997, 2003) but not to full-vehicle suspension yet. The main control objective is not only to improve the passengers comfort, but also to prevent the suspension travel from hitting its limitation. In this paper, the nonlinear backstepping control strategy is proposed to improve the inherent tradeoff between ride comfort of passengers and suspension travel. Our simulation results show that the vertical and angular motion of the vehicle body has been simultaneously minimized to improve ride quality of passenger. The remainder of the paper is organized as follows. In Section 2, we introduce the model of full-vehicle suspension system and analyze its system dynamics. In Section 3, the nonlinear backstepping design strategy is utilized to design an active suspension system for achieving our control objectives. In Section 4, some comparative simulation results including a passive suspension system and our resulting active suspension are illustrated. Finally, some concluding remarks are in Section 5 for further research.

2. SYSTEM MODEL AND DYNAMICS

The model of a full-vehicle suspension system proposed in Chalasani (1996); Ikenaga (2000) is shown in Fig. 1. The full-vehicle suspension model is represented as a nonlinear seven degree of freedom (DOF) system. It consists of a single sprung mass (vehicle body) connected to four unsprung masses (front-right, front-left, rear-right and

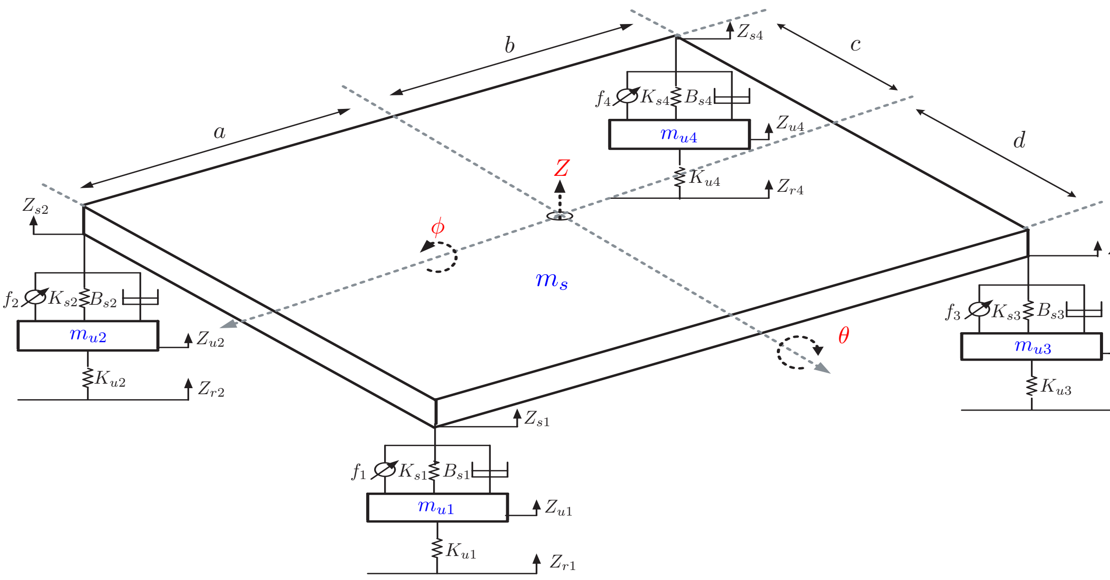

Fig. 1. Full-vehicle suspension system model

rear-left wheels) at each corner. The sprung mass is free to heave, pitch and roll, while the unsprung masses are free to bounce vertically with respect to the sprung mass. The suspension between the sprung mass and the unsprung masses are modeled as linear viscous dampers and spring elements, while the tires are modeled simple linear springs without damping.

By applying Newton's second law and using the static equilibrium position as the origin for the displacement of the center of gravity and angular the displacement of the vehicle body, the equations of the motion for the system can be formulated. The equation of motion for heave is represented as follows:

$$\begin{aligned}\ddot{Z} = \frac{1}{m_s}\Big\{ &- (K_{s1}+K_{s2}+K_{s3}+K_{s4})Z - f_1 - f_2 - f_3 \\ &- (B_{s1}+B_{s2}+B_{s3}+B_{s4})\dot{Z} + K_{s1}Z_{u1} + B_{s1}\dot{Z}_{u1} \\ &+ \big[-a(K_{s1}+K_{s2}) + b(K_{s3}+K_{s4})\big]\sin\theta + K_{s2}Z_{u2} \\ &+ \big[-a(B_{s1}+B_{s2}) + b(B_{s3}+B_{s4})\big]\dot{\theta}\cos\theta + B_{s2}\dot{Z}_{u2} \\ &+ \big[c(K_{s2}+K_{s4}) - d(K_{s1}+K_{s3})\big]\sin\phi + K_{s3}Z_{u3} \\ &+ \big[c(B_{s2}+B_{s4}) - d(B_{s1}+B_{s3})\big]\dot{\phi}\cos\phi + B_{s3}\dot{Z}_{u3} \\ &+ K_{s4}Z_{u4} + B_{s4}\dot{Z}_{u4} - f_4\Big\} \qquad (1)\end{aligned}$$

and the equation of the motion for pitch and roll is represented as follows:

$$\begin{aligned}I_\theta\ddot{\theta} = a\cos\theta\big[&K_{s1}(Z_{s1}-Z_{u1}) + B_{s1}(\dot{Z}_{s1}-\dot{Z}_{u1}) \\ &+ K_{s2}(Z_{s2}-Z_{u2}) + B_{s2}(\dot{Z}_{s2}-\dot{Z}_{u2}) - f_1 - f_2\big] \\ - b\cos\theta\big[&K_{s3}(Z_{s3}-Z_{u3}) + B_{s3}(\dot{Z}_{s3}-\dot{Z}_{u3}) \\ &+ K_{s4}(Z_{s4}-Z_{u4}) + B_{s4}(\dot{Z}_{s4}-\dot{Z}_{u4}) - f_3 - f_4\big] \qquad (2)\end{aligned}$$

$$\begin{aligned}I_\phi\ddot{\phi} = -c\cos\phi\big[&K_{s2}(Z_{s2}-Z_{u2}) + B_{s2}(\dot{Z}_{s2}-\dot{Z}_{u2}) \\ &+ K_{s4}(Z_{s4}-Z_{u4}) + B_{s4}(\dot{Z}_{s4}-\dot{Z}_{u4}) + f_2 + f_4\big] \\ + d\cos\phi\big[&K_{s1}(Z_{s1}-Z_{u1}) + B_{s1}(\dot{Z}_{s1}-\dot{Z}_{u1}) \\ &+ K_{s3}(Z_{s3}-Z_{u3}) + B_{s3}(\dot{Z}_{s3}-\dot{Z}_{u3}) + f_1 + f_3\big] \qquad (3)\end{aligned}$$

where m_s is the mass of the vehicle body and I_θ, I_ϕ are its centroidal moment of the inertia. With applying Newton's second law again on the front-left, front-right, rear-left and rear-right wheels un-sprung masses, the equations of the motion can also be formulated as follows:

- **Front-left wheel**

$$\begin{aligned}m_{u1}\ddot{Z}_{u1} = &K_{u1}(Z_{r1}-Z_{u1}) + K_{s1}(Z_{s1}-Z_{u1}) \\ &+ B_{s1}(\dot{Z}_{s1}-\dot{Z}_{u1}) + f_1 \qquad (4)\end{aligned}$$

- **Front-right wheel**

$$\begin{aligned}m_{u2}\ddot{Z}_{u2} = &K_{u2}(Z_{r2}-Z_{u2}) + K_{s2}(Z_{s2}-Z_{u2}) \\ &+ B_{s2}(\dot{Z}_{s2}-\dot{Z}_{u2}) + f_2 \qquad (5)\end{aligned}$$

- **Rear-left wheel**

$$\begin{aligned}m_{u1}\ddot{Z}_{u3} = &K_{u3}(Z_{r3}-Z_{u3}) + K_{s3}(Z_{s3}-Z_{u3}) \\ &+ B_{s3}(\dot{Z}_{s3}-\dot{Z}_{u3}) + f_3 \qquad (6)\end{aligned}$$

- **Rear-right wheel**

$$\begin{aligned}m_{u4}\ddot{Z}_{u4} = &K_{u4}(Z_{r4}-Z_{u4}) + K_{s4}(Z_{s4}-Z_{u4}) \\ &+ B_{s4}(\dot{Z}_{s4}-\dot{Z}_{u4}) + f_4 \qquad (7)\end{aligned}$$

The state assignment of system variables is assigned in the following:

$x_1 = Z$, is the ride height (heave)
$x_2 = \dot{Z}$, is the payload velocity
$x_3 = \theta$, is the pitch angle
$x_4 = \dot{\theta}$, is the pitch velocity
$x_5 = \phi$, is the roll angle
$x_6 = \dot{\phi}$, is the roll velocity
$x_7 = Z_{u1}$, is the front-left wheel unsprung height
$x_8 = \dot{Z}_{u1}$, is the front-left wheel unsprung velocity
$x_9 = Z_{u2}$, is the front-right wheel unsprung height
$x_{10} = \dot{Z}_{u2}$, is the front-right wheel unsprung velocity
$x_{11} = Z_{u3}$, is the rear-left wheel unsprung height
$x_{12} = \dot{Z}_{u3}$, is the rear-left wheel unsprung velocity
$x_{13} = Z_{u4}$, is the rear-right wheel unsprung height
$x_{14} = \dot{Z}_{u4}$, is the rear-right wheel unsprung velocity

The system state equations with these assigned state variables for the full-vehicle suspension system are as follows:

$$
\begin{aligned}
\dot{x}_1 =& x_2\\
\dot{x}_2 =& \frac{1}{m_s}\Big\{ -(K_{s1}+K_{s2}+K_{s3}+K_{s4})x_1 - f_1 - f_2 - f_3\\
& -(B_{s1}+B_{s2}+B_{s3}+B_{s4})x_2 - f_4 + K_{s1}x_7 + B_{s1}x_8\\
& +\big[b(K_{s3}+K_{s4}) - a(K_{s1}+K_{s2})\big]\sin x_3 + K_{s2}x_9\\
& +\big[b(B_{s3}+B_{s4}) - a(B_{s1}+B_{s2})\big]x_4\cos x_3 + B_{s2}x_{10}\\
& +\big[c(K_{s2}+K_{s4}) - d(K_{s1}+K_{s3})\big]\sin x_5 + K_{s3}x_{11}\\
& +\big[c(B_{s2}+B_{s4}) - d(B_{s1}+B_{s3})\big]x_6\cos x_5 + B_{s3}x_{12}\\
& + K_{s4}x_{13} + B_{s4}x_{14}\Big\}\\
\dot{x}_3 =& x_4\\
\dot{x}_4 =& \frac{\cos x_3}{I_\theta}\Big\{\big[-a(K_{s1}+K_{s2}) + b(K_{s3}+K_{s4})\big]x_1\\
& +\big[b(B_{s3}+B_{s4}) - a(B_{s1}+B_{s2})\big]x_2 - af_1\\
& -\big[a^2(K_{s1}+K_{s2}) + b^2(K_{s3}+K_{s4})\big]\sin x_3\\
& -\big[a^2(B_{s1}+B_{s2}) + b^2(B_{s3}+B_{s4})\big]x_4\cos x_3 + bf_2\\
& +\big[c(aK_{s2}-bK_{s4}) - d(aK_{s1}-bK_{s3})\big]\sin x_5 - af_3\\
& +\big[c(aB_{s2}-bB_{s4}) - d(aB_{s1}-bB_{s3})\big]x_6\cos x_5 + bf_4\\
& + aK_{s1}x_7 + aB_{s1}x_8 + aK_{s2}x_9 + aB_{s2}x_{10} - bK_{s3}x_{11}\\
& - bB_{s3}x_{12} - bK_{s4}x_{13} - bB_{s4}x_{14}\Big\}\\
\dot{x}_5 =& x_6\\
\dot{x}_6 =& \frac{\cos x_5}{I_\phi}\Big\{\big[c(K_{s2}+K_{s4}) - d(K_{s1}-K_{s3})\big]x_1\\
& +\big[c(B_{s2}+B_{s4}) - d(B_{s1}+B_{s3})\big]x_2 + df_1 - cf_2\\
& +\big[c(aK_{s2}-bK_{s4}) - d(aK_{s1}-bK_{s3})\big]\sin x_3\\
& +\big[c(aB_{s2}-bB_{s4}) + d(-aB_{s1}+bB_{s3})\big]x_4\cos x_3\\
& -\big[c^2(K_{s2}-K_{s4}) + d^2(-K_{s1}+K_{s3})\big]\sin x_5 + df_3\\
& -\big[c^2(B_{s2}-B_{s4}) + d^2(-B_{s1}+B_{s3})\big]x_6\cos x_5 - cf_4\\
& + dK_{s1}x_7 + dB_{s1}x_8 - cK_{s2}x_9 - cB_{s2}x_{10} + dK_{s3}x_{11}\\
& + dB_{s3}x_{12} - cK_{s4}x_{13} - cB_{s4}x_{14}\Big\}\\
\dot{x}_7 =& x_8\\
\dot{x}_8 =& \frac{1}{m_{u1}}[K_{u1}x_1 + B_{s1}x_2 + aK_{s1}\sin x_3 + aB_{s1}x_4\cos x_3\\
& + dK_{s1}\sin x_5 - (K_{u1}+K_{s1})x_7 - B_{s1}x_8 + K_{ul}Z_{r1}\\
& + dB_{s1}x_6\cos x_5 + f_1]\\
\dot{x}_9 =& x_{10}\\
\dot{x}_{10} =& \frac{1}{m_{u2}}[K_{u2}x_1 + B_{s2}x_2 + aK_{s2}\sin x_3 + aB_{s2}x_4\cos x_3\\
& - cK_{s2}\sin x_5 - (K_{u2}+K_{s2})x_9 - B_{s2}x_{10} + K_{u2}Z_{r2}\\
& - cB_{s2}x_6\cos x_5 + f_2]\\
\dot{x}_{11} =& x_{12}\\
\dot{x}_{12} =& \frac{1}{m_{u3}}[K_{u3}x_1 + B_{s3}x_2 - bK_{s3}\sin x_3 - bB_{s3}x_4\cos x_3\\
& + dK_{s3}\sin x_5 - (K_{u3}+K_{s3})x_{11} - B_{s3}x_{12} + K_{u3}Z_{r3}\\
& + dB_{s3}x_6\cos x_5 + f_3]\\
\dot{x}_{13} =& x_{14}\\
\dot{x}_{14} =& \frac{1}{m_{u4}}[K_{u4}x_1 + B_{s4}x_2 - bK_{s4}\sin x_3 - bB_{s4}x_4\cos x_3\\
& - cK_{s4}\sin x_5 - (K_{u4}+K_{s4})x_{13} - B_{s4}x_{14} + K_{u4}Z_{r4}\\
& - cB_{s4}x_6\cos x_5 + f_4]
\end{aligned}
\tag{8}
$$

3. ACTIVE SUSPENSION DESIGN

The control objective is not only to improve the ride quality for guaranteeing the passenger comfort, but also to prevent the suspension travel from hitting its limitation. The novelty is in use of the nonlinear filter whose effective bandwidth depends on the magnitudes of suspension travel. The new regulated variable is selected as follows:

$$z_1 = x_1 - \bar{\xi} \tag{9}$$

where $\bar{\xi}$ is a filter version of ξ

$$\bar{\xi}(s) = \frac{\epsilon_0 + \kappa\varphi(\zeta)}{s + \epsilon_0 + \kappa\varphi(\zeta)}\xi(s) \tag{10}$$

and ξ is defined as the linear combination of front-left, front-right, rear-left and rear-right wheel displacements, that is,

$$\xi = \kappa_1 x_7 + \kappa_2 x_9 + \kappa_3 x_{11} + \kappa_4 x_{13} \tag{11}$$

where $\kappa_i > 0$, for $i = 1, \ldots, 4$ and $\kappa_1+\kappa_2+\kappa_3+\kappa_4 = 1$. In (10), ϵ_0 and κ are the positive constant and the nonlinear function $\varphi(\zeta)$ illustrated in Fig. 2 is defined as follows:

$$\varphi(\zeta) = \begin{cases} (\dfrac{\zeta - m_1}{m_2})^2 \ , & \zeta > m_1 \\ 0 \ , & |\zeta| \le m_1 \\ (\dfrac{\zeta + m_1}{m_2})^2 \ , & \zeta < -m_1 \end{cases} \tag{12}$$

where $m_1 \ge 0$, $m_2 > 0$ and $\zeta = x_1 - \xi$ is the suspension travel.

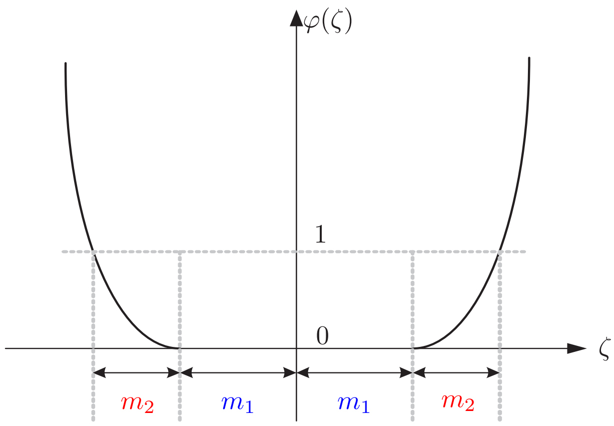

Fig. 2. Nonlinear function $\varphi(\zeta)$

The nonlinearity function which contains a deadzone is defined by the $-m_1 \le \zeta \le m_1$. While the suspension travel is smaller than m_1 in magnitude, the nonlinearity function remains dormant. In this region, the bandwidth of the nonlinear filter which is constant and equal to ϵ_0 can be selected to be small for satisfying the ride quality of passenger requirement. The nonlinear filter then becomes identical to the linear filter shown to possess good ride quality properties. As long as the suspension travel leaves this deadzone, the nonlinearity $\varphi(\zeta)$ is activated, and the effective bandwidth of nonlinear filter will be rapidly increased, therefore shifting the control objective to minimize the suspension travel. Hence, the introduction of the nonlinearity function with the control objective admits the controller to react diversely in different operating regions.

STEP 1: The derivative of z_1 is computed as

$$\dot{z}_1 = x_2 + \big(\epsilon_0 + \kappa\varphi(\zeta)\big)(\zeta - z_1) \tag{13}$$

And utilize the x_2 as the first virtual control variable, for which the stabilizing function is selected as

$$\alpha_1 = -c_1 z_1 - \big(\epsilon_0 + \kappa\varphi(\zeta)\big)\zeta \tag{14}$$

where c_1 is a positive design constant. The corresponding error state variable is defined as $z_2 = x_2 - \alpha_1$, and the resulting error equation is

$$\dot{z}_1 = -\big(c_1 + \epsilon_0 + \kappa\varphi(\zeta)\big)z_1 + z_2 \tag{15}$$

STEP 2: The derivative of z_2 is computed as

$$\begin{aligned}\dot{z}_2 = \frac{1}{m_s}\big\{ &-(K_{s1}+K_{s2}+K_{s3}+K_{s4})x_1 - f_1 - f_2 \\ &-(B_{s1}+B_{s2}+B_{s3}+B_{s4})x_2 + K_{s1}x_7 + B_{s1}x_8 \\ &+ [b(K_{s3}+K_{s4}) - a(K_{s1}+K_{s2})]\sin x_3 + K_{s3}x_{11} \\ &+ [b(B_{s3}+B_{s4}) - a(B_{s1}+B_{s2})]x_4\cos x_3 + B_{s3}x_{12} \\ &+ [c(K_{s2}+K_{s4}) - d(K_{s1}+K_{s3})]\sin x_5 + K_{s4}x_{13} \\ &+ [c(B_{s2}+B_{s4}) - d(B_{s1}+B_{s3})]x_6\cos x_5 + B_{s4}x_{14} \\ &+ K_{s2}x_9 + B_{s2}x_{10} - f_3 - f_4\big\} - c_1^2 z_1 + c_1 z_2 \\ &- c_1\big(\epsilon_0 + \kappa\varphi(\zeta)\big)z_1 + \big(\epsilon_0 + \kappa\varphi(\zeta)\big)\frac{d\zeta}{dt} + \kappa\zeta\frac{d\varphi}{d\zeta}\frac{d\zeta}{dt}\end{aligned} \tag{16}$$

Since the actual control inputs f_1, f_2, f_3 and f_4 appear in (16), the control laws are chosen as follows:

$$\begin{aligned}f_1 &= Q(x) + K_{s1}x_7 + B_{s1}x_8 \\ &\quad + \big[\big(\epsilon_0 + \kappa\varphi(\zeta)\big) + \kappa\zeta\frac{d\varphi}{d\zeta}\big]\big(\frac{1}{4}x_2 - \kappa_1 x_8\big) \\ f_2 &= Q(x) + K_{s2}x_9 + B_{s2}x_{10} \\ &\quad + \big[\big(\epsilon_0 + \kappa\varphi(\zeta)\big) + \kappa\zeta\frac{d\varphi}{d\zeta}\big]\big(\frac{1}{4}x_2 - \kappa_2 x_{10}\big) \\ f_3 &= Q(x) + K_{s3}x_{11} + B_{s3}x_{12} \\ &\quad + \big[\big(\epsilon_0 + \kappa\varphi(\zeta)\big) + \kappa\zeta\frac{d\varphi}{d\zeta}\big]\big(\frac{1}{4}x_2 - \kappa_3 x_{12}\big) \\ f_4 &= Q(x) + K_{s4}x_{13} + B_{s4}x_{14} \\ &\quad + \big[\big(\epsilon_0 + \kappa\varphi(\zeta)\big) + \kappa\zeta\frac{d\varphi}{d\zeta}\big]\big(\frac{1}{4}x_2 - \kappa_4 x_{14}\big)\end{aligned} \tag{17}$$

where

$$\begin{aligned}Q(x) = \frac{1}{4}\big\{ &-(K_{s1}+K_{s2}+K_{s3}+K_{s4})x_1 \\ &-(B_{s1}+B_{s2}+B_{s3}+B_{s4})x_2 \\ &+ [b(K_{s3}+K_{s4}) - a(K_{s1}+K_{s2})]\sin x_3 \\ &+ [b(B_{s3}+B_{s4}) - a(B_{s1}+B_{s2})]x_4\cos x_3 \\ &+ [c(K_{s2}+K_{s2}) - d(K_{s1}+K_{s3})]\sin x_5 \\ &+ [c(B_{s1}+B_{s4}) - d(B_{s1}-B_{s1})]x_6\cos x_5\big\} \\ &+ \frac{1}{4}m_s\big[z_1 - c_1^2 z_1 - c_1\big(\epsilon_0 + \kappa\varphi(\zeta)\big)z_1\big]\end{aligned}$$

and c_2 is a positive design constant. Therefore, the derivation of z_2 becomes in the following:

$$\dot{z}_2 = -z_1 - c_2 z_2 \tag{18}$$

After finishing the procedure of nonlinear backstepping design with two steps, now let us consider the following Lyapunov function for the analysis of system stability:

$$V = \frac{1}{2}z_1^2 + \frac{1}{2}z_2^2 \tag{19}$$

From (15)-(18), the derivative of (19) is calculated as

$$\dot{V} = -\big[c_1 + \big(\epsilon_0 + \kappa\varphi(\zeta)\big)\big]z_1^2 - c_2 z_2^2 < 0 \tag{20}$$

According to the Lyapunov stability theorem, it implies that the error system is globally exponentially stable. Alternative stability analysis can be done by writing the resulting closed-loop error system as follows:

$$\begin{bmatrix}\dot{z}_1 \\ \dot{z}_2\end{bmatrix} = \begin{bmatrix}-c_1 - \big(\epsilon_0 + \kappa\varphi(\zeta)\big) & 1 \\ -1 & -c_2\end{bmatrix}\begin{bmatrix}z_1 \\ z_2\end{bmatrix} \tag{21}$$

It is clear to show that the 2×2 square matrix is Hurwitz, so the error system has a globally exponentially stable at equilibrium point. This is true with any positive constants for c_1 and c_2, although very small values of constants may lead to unacceptably large errors. Moreover, under our investigation of zero dynamics, the resulting closed-loop system is also stable. That is to say, the displacement of the center of gravity is indeed minimized to achieve our desired control objective for improving the ride comfort of passengers without any unacceptable wheel oscillations.

4. SIMULATION RESULTS

The model of full-vehicle suspension system is shown in Fig. 1. The parameters of full-vehicle model for this paper are given as follows:

Table 1. System parameter values

Parameter	Value	Parameter	Value
m_{u1}	59 kg	m_{u2}	59 kg
m_{u3}	59 kg	m_{u3}	59 kg
K_{s1}	35000 N/m	K_{s2}	35000 N/m
K_{s3}	38000 N/m	K_{s4}	38000 N/m
B_{s1}	1000 N/m	B_{s2}	1000 N/m
B_{s3}	1100 N/m	B_{s4}	1100 N/m
K_{u1}	190000 N/m	K_{u2}	190000 N/m
K_{u3}	190000 N/m	K_{u4}	190000 N/m
a	1.4 m	b	1.7 m
c	1 m	d	2 m
m_s	1500kg	I_θ	2160 kgm^2
I_ϕ	460 kgm^2		

Let the road disturbances employed on the front-left, front-right, rear-left and rear-right wheels be:

$$Z_{r1}(t) = Z_{r2}(t) = \mu_r\big(1 - \cos(8\pi t)\big),\ 0.5 \le t \le 0.75$$
$$Z_{r3}(t) = Z_{r4}(t) = \mu_r\big(1 - \cos(8\pi t)\big),\ 3.0 \le t \le 3.25$$

where μ_r is the amplitude (meters). The other simulation parameters with nonlinear filter design are as follows:

- Simulation time: 10 seconds.
- Suspension travel limitation: ± 12 cm.

Table 2. Design constants

Design Constant	Value	Design Constant	Value
ϵ_0	1.5	κ	0.0165
m_1	0.015	m_2	0.005
c_1	1	c_2	1
κ_1	0.25	κ_2	0.25
κ_3	0.25	κ_4	0.25

The results are able to certify the utility of the nonlinear backstepping controller by comparing our backstepping active suspension design (solid line) with active suspension with linear filter (dotted line) and a standard passive suspension (dashed line). The simulation results are shown in two kinds of diverse consequences with the different choice of road bump height: (I) μ_r = 0.025 and (II) μ_r = 0.06.

(I) Road bump height with μ_r = 0.025:

The plots of displacement and acceleration of body center, pitch angle and its acceleration, roll angle and its acceleration are shown in Fig. 3. The plots of front-left and rear-right suspension travel and wheel displacement are shown in Fig. 4. While the road bump height is 5 cm, the suspension travel is smaller than m_1 in magnitude. In that region, the nonlinear filter becomes identical to the linear filter shown to possess good ride quality properties. Therefore, the simulation results shown in Fig. 3 indeed verify that our active suspension design here possesses potentials to simultaneously minimize the displacement and acceleration of heave, pitch and roll motions for guaranteeing the improvement of ride quality.

(II) Road bump height with μ_r = 0.06:

The plots of displacement and acceleration of body center, pitch angle and its acceleration, roll angle and its acceleration are shown in Fig. 5. In addition, Fig. 6 illustrates the front-left and rear-right suspension travel and wheel displacement. A further increase in the height of road bump reaches to 12 cm. The suspension travel leaves this deadzone. The nonlinearity $\varphi(\zeta)$ is activated to shift the restraint of suspension travel. According to Fig. 6, the active suspension design with nonlinear filter is the one which does not hit its suspension travel limitation. As the result, the backstepping design with nonlinear filter exactly has the ability to improve the tradeoff between ride quality and suspension travel. Therefore, it can behave to deal with the conflicting control objectives in different operating regions.

5. CONCLUDING REMARKS

In this paper, the nonlinear backstepping control strategy has been proposed for the control of full-vehicle active suspension systems. The main control objective is not only to improve the ride quality, but also to prevent the suspension travel from hitting its limitation. According to the simulation results, the active suspension design has clearly demonstrated that the nonlinear controllers possess potentials to improve the two conflicting control objectives which are passenger comfort and suspension travel. In the future researches, while the road-adaptive and modular adaptive backstepping control design proposed in Lin (1996, 1997) have been well developed in active suspension with quarter-car model, we are interested in extending these design methods to the full-vehicle active suspension systems. Furthermore, the novel conception is the coordination design of four active suspensions. If the mutual coordination among all active suspensions can be achieved, then the passenger comfort will be capable of being strongly enhanced because reduction of vertical acceleration at each end has been guaranteed.

REFERENCES

R. M. Chalasani and B. Soenarko, "Ride performance potential of the active suspension system - Part II: comprehensive analysis based on the full-vehicle model," *ASME Symposium on Simulation and Control of the Ground Vehicles and Transportation Systems,* Anaheim CA, 1996, pp. 205-234.

E. Esmailzadeh and H. D. Taghirad, "Active vehicle suspensions with optimal state-feedback Control," *International Jorunal of Mechanical Science,* pp. 137-151, Jun. 1996.

C.-J. Huang and J.-S. Lin, "Nonlinear active suspension control design applied to a half-car model," *Proceedings of 2004 IEEE International Conference on Networking, Sensing and Control*, Taipei, Taiwan, March, 2004, pp. 719-724.

S. Ikenaga, F. L. Lewis, J. Campos and L. Davis, "Active suspension control of the ground vehicle based on a full-vehicle model," *Proceeding of 2000 IEEE on American Control Conference,* vol. 6, pp. 4019-4024, 2000.

D. Karnopp, "Passive and active suspension control of the road vehicle heave and pitch motion," *IFAC 10th Triennal World Congress,* pp. 183-188, Sept. 1992.

J.-S. Lin and I. Kanellakopoulos, "Adaptive nonlinear control in active suspensions," *Preprints of the 13th World Congress of International Federation of Automatic Control,* San Francisco, CA, July 1996, vol. F, pp. 341-346.

J.-S. Lin and I. Kanellakopoulos, "Road-adaptive nonlinear control of active suspension," *Proceedings of the 1997 American Control Conference,* Albuquerque, NM, June 1997, pp. 714-718

J.-S. Lin and I. Kanellakopoulos, "Modular adaptive design for active suspensions," *Proceedings of the 36th IEEE Conference on Decision and Control,* San Diego, CA, December 1997, pp. 3626-3631.

J.-S. Lin and I. Kanellakopoulos, "Nonlinear design of active suspensions," *IEEE Control Systems Magazine*, pp. 45-59, June 1997.

J.-S. Lin and C.-J. Huang, "Nonlinear backstepping control design of half-car active suspension systems," *International Journal of Vehicle Design,* vol. 33, no. 4, pp. 332-350, 2003.

J.-S. Lin and C.-J. Huang, "Nonlinear backstepping active suspension design applied to a half-car model," *Vehicle System Dynamics*, vol. 42, no. 6, pp. 373-393, 2004.

J.-S. Lin and W.-E. Ting, "Nonlinear control design of anti-lock braking systems with assistance of active suspension," *IET Control Theory & Applications*, vol. 1, no. 1, pp. 343-348, 2007.

L. R. Miller, "Tuning passive, semi-active, and active suspension system," *Proceedings of 27th IEEE on Decision and Control,* pp. 2047-2053, Jun. 1988.

J. J. H. Paulides, L. Encica, E. A. Lomonova and A. J. A. Vandenput, "Design considerations for semi-active electromagnetic suspensions," *IEEE Transactions on Magnetics,* vol. 42, pp. 3446-3448, Oct. 2006.

Y. M. Sam and N. Ahmad, "LQR controller for active suspension system," *Proceedings of the 2000 IEEE Conference on Control Applications,* Sept. 2000.

A. G. Thompson and C. E. M. Pearce, "Direct computation of performance index for an optimally controlled active suspension system with preview applied to a half vehicle model," *Vehicle System Dynamics,* vol. 35, no. 2, pp. 121-137, 2001.

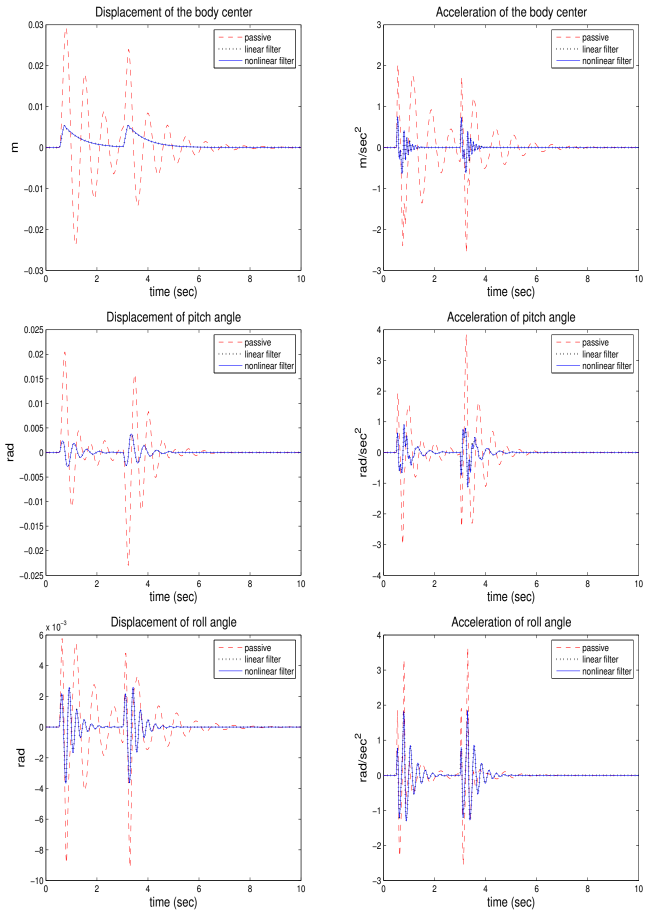

Fig. 3. The response of heave, pitch and roll with road bump height 5 cm

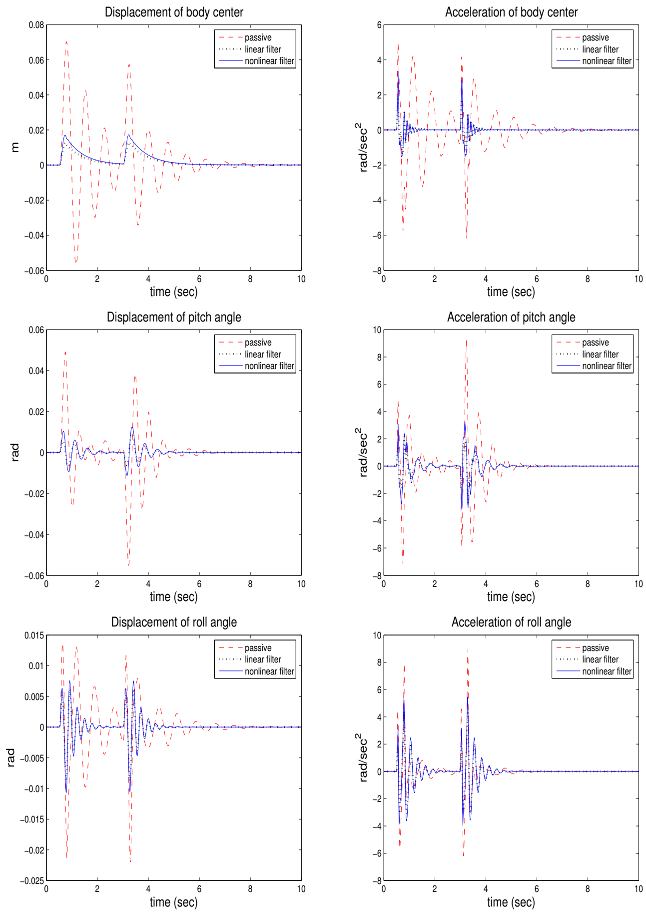

Fig. 5. The response of heave, pitch and roll with road bump height 12 cm

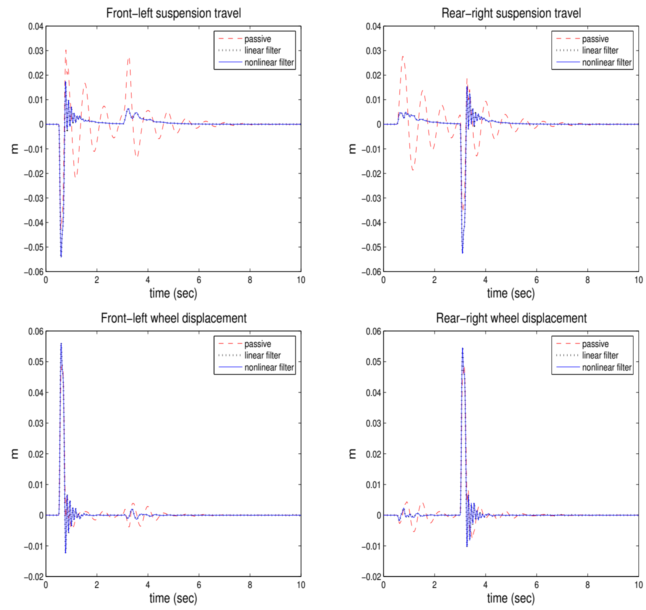

Fig. 4. The response of front-left and rear-right suspension and wheel with road bump height 5 cm

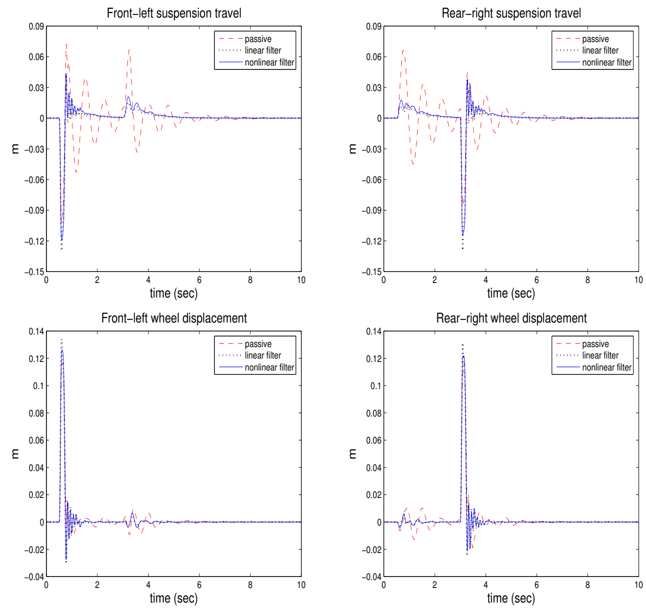

Fig. 6. The response of front-left and rear-right suspension and wheel with road bump height 12 cm